

# Kinetic Spectroscopy in the Far Vacuum Ultraviolet

## Part 2.—Fluorine Atom Resonance Spectrometry and the Measurement of $F^2P$ Atom Concentrations

BY PETER P. BEMAND AND MICHAEL A. A. CLYNE\*

Department of Chemistry, Queen Mary College, Mile End Road, London E1 4NS

*Received 9th May, 1975*

A technique for the first atomic resonance detection of ground state  $F 2p^5\ ^2P_J$  atoms in a flow system is described. Collimated hole structures were used in place of windows to separate the lamp, flow tube and spectrometer. Resonance absorption measurements of the  $3s-2p^5$  multiplet transition of F, between 95 and 98 nm, were used to obtain the first values for the oscillator strengths  $f_{ik}$  of the 97.39 nm  $^4P_{3/2}-^2P_{3/2}$  and the 97.77 nm  $^4P_{3/2}-^2P_{1/2}$  lines of these multiplets. The values, which have an estimated standard error of  $\pm 30\%$ , are:  $f_{ik}(97.39) = 4 \times 10^{-5}$ ;  $f_{ik}(97.77) = 1 \times 10^{-5}$ .

Fluorine atom resonance fluorescence in the  $3s\ ^2P_J-2p^5\ ^2P_J$  multiplet, and in one line of the  $3s\ ^4P_J-2p^5\ ^2P_J$  multiplet, was observed for the first time; it was used to measure concentrations of  $F^2P_J$  atoms down to  $1 \times 10^{11}\text{ cm}^{-3}$ . Measurement of absolute  $[F^2P_J]$  was by means of the rapid reactions (1) and (2),



Attenuation of F atom resonance fluorescence was used to measure the rate constant  $k_1$  at 300 K. Combining this value with another (mass spectrometric) determination of  $k_1$ , the mean value  $k_1 = (2.2 \pm 1.1) \times 10^{-10}\text{ cm}^3\text{ molecule}^{-1}\text{ s}^{-1}$  from 298 to 300 K was obtained.

Although ground state fluorine atoms may be directly detected and determined by e.p.r. spectrometry,<sup>1</sup> mass spectrometry<sup>2-4</sup> and atomic resonance spectrometry,<sup>5</sup> few reliable kinetic studies of elementary reactions of  $F^2P_J$  atoms have been reported until recently. There are several major problems: (i) a satisfactory source of  $F^2P_J$  atoms, (ii) the rapidity of most reactions of  $F^2P_J$ , even at 298 K, which requires high sensitivity of detection and/or rapid time response of the kinetic technique, (iii) mechanistic complications due to rapid secondary reactions, particularly in the case of hydrogen-containing reactants, and (iv) the irreproducibility of surface reactions of F atoms.

At present, problem (i), the requirement for a satisfactory source of  $F^2P_J$  atoms, restricts available kinetic techniques to the discharge-flow method. In this method, the simplest source of  $F^2P_J$  is a microwave discharge in dilute  $F_2 + \text{He}(\text{Ar})$  mixtures,<sup>6</sup> whilst similar discharges in  $CF_4$  or  $SF_6$  have also been used.<sup>7</sup> The sensitivity of e.p.r. spectrometry at present is probably insufficient for systematic kinetic studies of  $F^2P_J$ , which has effectively restricted such studies to mass spectrometry in a discharge-flow system. The use of  $\text{NO} + \text{F}$  chemiluminescence<sup>7</sup> appears promising, although the precursor of that chemiluminescence still remains to be positively identified as FNO. It remains to be seen whether the sensitivity of the  $\text{NO} + \text{F}$  technique is adequate for kinetic measurements of very rapid bimolecular rate constants.

We therefore attempted to develop a technique for systematic kinetic measurements of  $F^2P_J$  atom reactions using atomic resonance spectrometry, preferably in fluorescence rather than in absorption, to determine  $F^2P_J$  atom concentrations. The

experimental problems are compounded by the necessity to work in the far vacuum ultraviolet near 95 nm, below the shortest wavelength (105 nm) possible with windows. However, our attempts were largely successful, and  $F^2P_J$  atoms were detected by atomic resonance fluorescence at concentrations down to  $1 \times 10^{11} \text{ cm}^{-3}$ . We were able to establish a value for the rate constant of the  $F + Br_2$  reaction near 298 K. Reactions of F with  $Cl_2$ ,<sup>4, 8, 9</sup>  $Br_2$ ,<sup>9</sup>  $I_2$ <sup>9</sup> and  $ICl$ <sup>9</sup> all proceed at rates close to the hard-sphere bimolecular collision frequency at 298 K. It will be possible to make extensive direct measurements of the rate constants for somewhat slower reactions than these, using a resonance fluorescence technique similar to that described here.

## EXPERIMENTAL

A system for atomic resonance fluorescence studies of atoms generated in a low-pressure discharge flow system has been described previously.<sup>10, 11</sup> The present flow system was similar to the previous ones,<sup>10, 11</sup> but important modifications were necessary to allow the detection of radiation near 95 nm where all solid window materials absorb strongly. The following account emphasizes these modifications.

### PRODUCTION OF FLUORINE $F^2P_J$ ATOMS

A 2.45 GHz discharge in  $F_2 + He$  or  $F_2 + Ar$  mixtures in an uncoated silica tube (10 mm i.d.) was used as the source of  $F^2P_J$  atoms.  $F_2$  was obtained as a mixture (4 mol %) with helium and was used direct from the cylinder, except for the addition of further dry He or Ar diluent. The typical degree of dissociation of  $F_2$  was 0.8, and it was insensitive to incident discharge power.<sup>4</sup> The major impurity in the dissociated  $F_2$  was  $SiF_4$ ,<sup>3, 4</sup> which arises mainly from attack on the  $SiO_2$  discharge tube.<sup>4</sup> Oxygen atoms,  $O^3P_J$ , were also detected, using atomic resonance spectrometry at  $\lambda$  130.2 nm. Use of a discharge bypass for production of low F atom concentrations led to typical  $O^3P_J$  impurity atom concentrations around  $2 \times 10^{11} \text{ cm}^{-3}$  under conditions where  $[F] \approx 1 \times 10^{12} \text{ cm}^{-3}$  and  $[He] \approx 5 \times 10^{16} \text{ cm}^{-3}$ . These relatively high  $O^3P_J$  atom concentrations are thought to arise from partial dissociation of  $O_2$  liberated in the attack by fluorine or fluorine atoms on the  $SiO_2$  material of the discharge tube. The reaction,  $O + F_2 \rightarrow FO + F$ , is slow at 298 K; therefore  $O^3P_J$  atoms are not scavenged by undissociated  $F_2$ , and persist as a major impurity in the  $F + F_2$  stream. However atomic hydrogen could not be detected under the same conditions, from which an upper limit  $[H] \leq 1 \times 10^{11} \text{ cm}^{-3}$  is derived.

For the determination of F atom concentrations, the  $F + Br_2$  and  $F + Cl_2$  reactions were used. To avoid the use of the necessarily very low flow rates of pure halogens required to measure  $[F]$  as low as  $10^{12} \text{ cm}^{-3}$ , larger flows ( $\sim 10^{18} \text{ molecule s}^{-1}$ ) of dilute mixtures of  $Br_2$  or  $Cl_2$  ( $\sim 1 \text{ mol } \%$ ) with argon were used. The mole fraction of the halogen in these mixtures was measured by absorption spectrometry at 414 nm ( $Br_2$ ) or 350 nm ( $Cl_2$ ).

### DETECTION OF FLUORINE ATOMS BY ATOMIC RESONANCE SPECTROMETRY

The source of F atom resonance radiation,  $3s-2p^5$ , which was a microwave discharge in  $F_2 + He$  mixtures, has been described.<sup>5</sup> Three collimated hole structures (CHS) were used to separate this lamp from the flow tube and the vacuum spectrometer (fig. 1). The CHS, consisting of a stainless steel grid of many parallel channels, 0.1 mm in diameter and 1 mm long, had a light transmission of 40 %, but showed a low gas conductance. Having an aperture of about  $f/10$ , CHS offer a considerable advantage in light gathering power over the long capillaries conventionally used to separate source, absorber and spectrometer in far vacuum ultraviolet spectroscopy. Fig. 1 shows the four distinct regions of the windowless detection system; the lamp L, the flow tube R, the buffer chamber B and the spectrometer V, with each pair separated by a CHS, C. To minimize diffusional mixing of the regions, argon (rather than helium) was used where possible, and the total pressure in all four regions was as high as possible. The upper limit was set by the maximum gas load that could be handled by the spectrometer diffusion pump (at spectrometer pressure  $p_V$ ) without stalling, and by the fall in lamp intensity with increase in lamp pressure,  $p_L$ . The

pressure in the buffer chamber  $p_B$  was slightly greater than that in the flow tube  $p_R$  to prevent F or  $F_2$  entering the spectrometer. Also,  $p_L$  was always greater than  $p_R$  to prevent F or  $F_2$  diffusing from the flow tube into the lamp, which would invalidate the atomic resonance results. The typical pressure parameters thus adopted were:  $p_L = 400$ ,  $p_R = 220$ ,  $p_B = 310$  and  $p_V = 0.1 \text{ N m}^{-2}$ . Net flow into the flow tube from the lamp and from the buffer chamber could not be entirely prevented, and the above typical conditions led to an increase in flow rate of  $50 \mu\text{mol s}^{-1}$  due to the lamp and buffer chamber together. This was equivalent

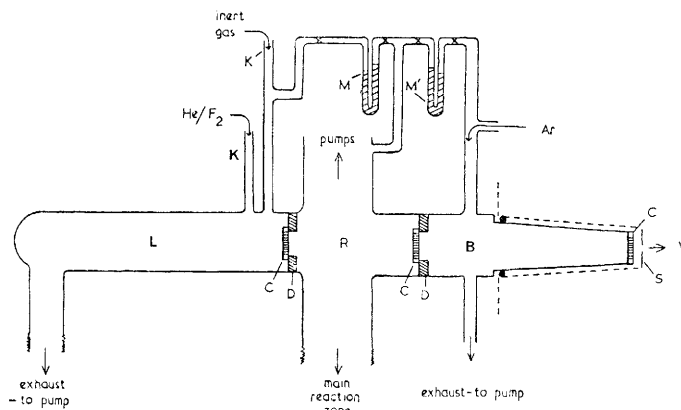


FIG. 1.—Windowless system for resonance spectrometry of  $F^2P_J$  atoms. B, buffer chamber; C, collimated hole structures, two of which were mounted on specially-fabricated glass discs; D; K, inlet to lamp L; M,  $M^1$ , differential manometers; R, section of flow tube; S, spectrometer slit, sealed via an O-ring seal to the silica apparatus; V, vacuum spectrometer.

to an increase of about 6 % in total mass flow rate in the flow tube. An uncertainty in the atom and reagent concentrations, and in the linear flow velocity, of the order of 6 % was thereby introduced, leading in turn to an uncertainty in derived second order rate constants of about  $\pm 12$  %. Replacement of the CHS with 0.1 mm diameter holes by other CHS with 0.02 or 0.01 mm holes would be advantageous in reducing diffusional mixing still further. (However, this would inevitably lead to some loss in detected photon flux).

The flow tube was provided with large pumps, ( $\sim 17 \text{ l s}^{-1}$  nominal displacement) giving a maximum linear flow velocity of  $2000 \text{ cm s}^{-1}$ , whilst two small rotary pumps were used for the lamp flow and for the buffer volume flow. The spectrometer was pumped by a baffled 10 cm oil diffusion pump, having an actual speed of  $80 \text{ l s}^{-1}$ , backed by a rotary pump ( $2.5 \text{ l s}^{-1}$ ).

The spectrometer, a 1 m normal-incidence mounting (Hilger E760), was provided with a concave aluminized replica grating overcoated with Pt ( $56 \times 96 \text{ mm}$ ),  $600 \text{ line mm}^{-1}$ , blazed at  $90 \text{ nm}$  in the first order (Bausch and Lomb). The detector was an E.M.I. 9789QA photomultiplier cell whose end (silica) window was coated with sodium salicylate as a phosphor. A photon counting system was used to detect and record individual photoelectrons. The photomultiplier cell showed a counting plateau at around  $1000 \text{ V e.h.t.}$  overall, at which potential its dark count rate was about  $20 \text{ Hz}$ . However, it was found that with a reduction of e.h.t. to  $850 \text{ V}$ , the dark count rate of this particular photomultiplier fell to  $2.5 \text{ Hz}$ , whilst the corresponding photon count rate was still two-thirds of that observed at  $1000 \text{ V}$ . It appears that, at a given e.h.t., the mean pulse height due to dark electrons was less than that due to photoelectrons originating at the photocathode. The photomultiplier cell was cooled with circulating water from room temperature, typically  $299 \text{ K}$ , to that of the laboratory water tank ( $290 \text{ K}$ ), leading to a further useful reduction in mean dark count rate from  $2.5$  to  $1.5 \text{ Hz}$  at  $850 \text{ V}$ . This method of using the photomultiplier, leading to an unusually low dark count, was essential to the measurement of the very low photon count rates due to F atom fluorescence encountered in our work. The advantage of the low dark count of the

Fig. 3 shows a spectrum of the main  $3s-2p^5$  lines, obtained with the best available resolution of 0.04 nm, together with the remaining (much weaker) F atom lines observed between 58.4 and 95 nm. After the  $3s-2p^5$  multiplet, the next most intense feature was a doublet ( $\lambda$  80.70, 80.96 nm), due to the  $3s'(^1D) \ ^2D_{\frac{3}{2},\frac{5}{2}}-2p^5 \ ^2P_{\frac{3}{2}}$  and  $3s'(^1D) \ ^2D_{\frac{3}{2}}-2p^5 \ ^2P_{\frac{1}{2}}$  transitions (fig. 2). A very weak, but well-defined multiplet due to the  $4s \ ^2P_J-2p^5 \ ^2P_J$  transition of F, between 79.00 and 79.44 nm, was also identified in fig. 3.

The relative intensities of the  $3s-2p^5$ ,  $3s'(^1D)-2p^5$  and  $4s-2p^5$  transitions of F in the resonance lamp parallel those of the analogous  $4s-3p^5$ ,  $4s'(^1D)-3p^5$  and  $5s-3p^5$  transitions of Cl emitted from a similar Cl lamp.<sup>19</sup> In fact, the background spectrum in the chlorine resonance lamp was too intense to permit unequivocal identification of the very weak  $5s-3p^5$  lines of Cl near 109 nm.

However, only the first  $3s-2p^5$  multiplet transitions of F were intense enough for resonance fluorescence studies of  $F\ 2p^5\ ^2P_J$  atoms, unlike the situation for  $Cl\ 3p^5\ ^2P_J$  atoms, where the  $4s'(^1D)-3p^5$ , as well as the  $4s-3p^5$  transition, is intense enough for detection of Cl atom fluorescence.<sup>19</sup>

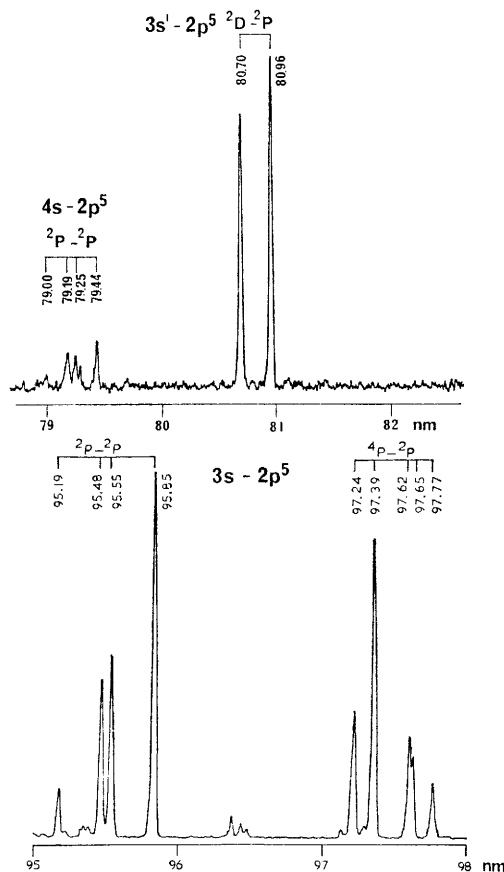


FIG. 3.—Emission spectrum of F atom resonance lamp.  $F_2$  (1 mol %)+He, 25 W incident microwave power. Lower spectrum is that of the intense  $^2P_J-^2P_J$  multiplets of the  $3s-2p^5$  transitions using  $5\ \mu\text{m} \times 10\ \text{mm}$  slits. Detected photon flux rate at 95.85 nm = 1.8 kHz. Upper spectrum shows the much weaker  $3s'\ ^2D_J-2p^5\ ^2P_J$  and  $4s\ ^2P_J-2p^5\ ^2P_J$  multiplets, using  $13\ \mu\text{m} \times 10\ \text{mm}$  slits. Detected photon count at 80.70 nm = 50 Hz. Note that the lamp spectrum shows negligible continuum background. Noise (photomultiplier dark count + scattered light) count rate = 2.5 Hz.

#### MEASUREMENT OF $F\ ^2P_J$ CONCENTRATIONS

Methods based on rapid "titration" reactions<sup>12</sup> for the measurement of absolute fluorine atom concentrations have been reviewed [e.g., ref. (4) and references therein]. Reaction (2),



has been used for this purpose in mass spectrometric kinetic studies of F atom reactions.<sup>4, 9</sup> Either the concentration of Cl<sub>2</sub> removed, or the concentration of ClF formed,<sup>9</sup> in reaction (2), was used to measure [F]. Reaction (2) proceeds at a rate approaching the hard-sphere bimolecular collision frequency at 298 K with  $k_2^{298}$  reported to be  $0.86 \times 10^{-10}$ ,<sup>8</sup>  $(1.1 \pm 0.3) \times 10^{-10}$ <sup>4</sup> and  $(1.6 \pm 0.5) \times 10^{-10}$  cm<sup>3</sup> molecule<sup>-1</sup> s<sup>-1</sup>.<sup>9</sup> Since the possible secondary step, Cl + F<sub>2</sub> → ClF + F, is believed to be slow [ $k^{298} < 5 \times 10^{-14}$  cm<sup>3</sup> molecule<sup>-1</sup> s<sup>-1</sup> (ref. (13) and this work)], reaction (2) is a nearly ideal titration reaction for F. However, careful consideration of the nearly-balanced thermochemistry of reaction (2) is necessary. In the following discussion, the major reacting species is taken to be F <sup>2</sup>P<sub>3/2</sub>, since F <sup>2</sup>P<sub>3/2</sub> accounts for only 7 % of Σ[F] in a Boltzmann distribution at 298 K.

Coxon<sup>14</sup> has reviewed the dissociation energies<sup>16</sup> of ClF, BrF and IF, and he concluded that  $D_0^\circ$  (ClF) definitely lies between the limits 246.7 and 252.4 kJ mol<sup>-1</sup>. As he pointed out, recent measurements of the equilibrium constant for reaction (2),<sup>15</sup> proceeding presumably mainly to Cl <sup>2</sup>P<sub>3/2</sub>, support the higher value of 252.4 kJ mol<sup>-1</sup> for  $D_0^\circ$  (ClF). A short extrapolation (from 306 K) of the results of Nordine<sup>15</sup> gave  $K_{2eq} = (355 \pm 50)$  for reaction (2) at 298 K. The absolute minimum value for  $K_{2eq}$ , based on the (less likely) value  $D_0^\circ$  (ClF) = 246.7 kJ mol<sup>-1</sup>, is  $K_{2eq} > (5.1 \pm 0.8)$  at 298 K. Even this low value for  $K_{2eq}$  is sufficient to give ≥ 90 % reaction in studies, such as those cited,<sup>4, 9</sup> where a considerable excess of either F, or of Cl<sub>2</sub>, was present

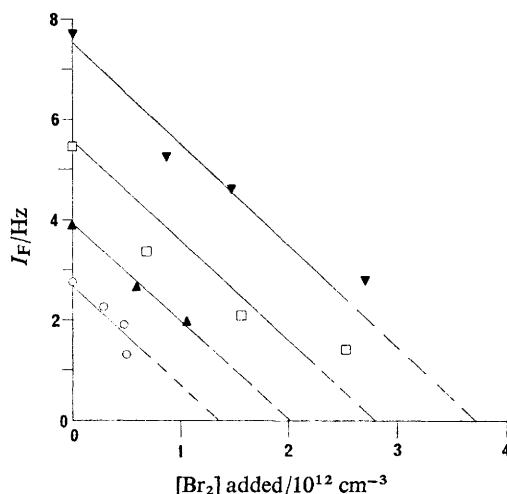
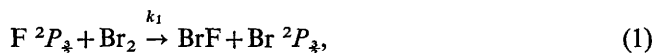


FIG. 4.—F + Br<sub>2</sub> titration for the measurement of [F]. Plot shows the variation of F <sup>2</sup>P<sub>J</sub>–<sup>2</sup>P<sub>J</sub> fluorescence intensity with [Br<sub>2</sub>] added. Note that for complete reaction [F] = [F]<sub>0</sub> – ([Br<sub>2</sub>] added), where [F]<sub>0</sub> is the abscissa intercept corresponding to the F + Br<sub>2</sub> titration endpoint.

in the F + Cl<sub>2</sub> reaction. However, in a conventional titration,<sup>12</sup> where approximately equal initial concentrations of reagents are used to give an endpoint, i.e., [F]<sub>0</sub> ~ [Cl<sub>2</sub>]<sub>0</sub>, the reaction (2) would proceed to only ~70 % completion if  $K_{2eq}$  is as low as 5.1.

Reaction (1),



is an alternative titration reaction for F, with  $k_1^{298}$  reported to be  $(3.1 \pm 0.9) \times 10^{-10}$  cm<sup>3</sup> molecule<sup>-1</sup> s<sup>-1</sup>.<sup>9</sup> As in the case of  $D_0^\circ$  (ClF), the upper and lower limits for  $D_0^\circ$  (BrF) are well defined, in this case as  $261.4 \geq D_0^\circ$  (BrF)  $\geq 245.6$  kJ mol<sup>-1</sup>.<sup>14</sup> Using  $D_{298}^\circ$  (Br<sub>2</sub>) = 192.9 kJ mol<sup>-1</sup>, the absolute minimum value for  $K_{1eq}$  is 10<sup>9</sup> at

298 K. Reversibility of reaction (1) is therefore not a problem in F atom titrations with  $\text{Br}_2$ .

In this work, both reactions (1) and (2) have been used to measure absolute F atom concentrations. The intensity,  $I_F$ , of F atom resonance fluorescence (see below) was used to monitor relative  $[\text{F}]$ . Usually, a simple titration of  $\text{F } ^2P_J$  atoms with  $\text{Br}_2$  was carried out, estimating the endpoint to be critical extinction of the F atom fluorescence. Since it was never practicable (for our kinetic studies) to use initial F concentrations less than  $1 \times 10^{12} \text{ cm}^{-3}$ , and since  $k_1$  is reported to be  $(3.1 \pm 0.9) \times 10^{-10} \text{ cm}^3 \text{ molecule}^{-1} \text{ s}^{-1}$ ,<sup>9</sup> the typical reaction time of 10 ms would be sufficient to ensure >95 % completion of the  $\text{F} + \text{Br}_2$  reaction. In studies using relatively low  $[\text{F}]$ , not much greater than  $1 \times 10^{12} \text{ cm}^{-3}$ , it was advantageous to obtain endpoints by extrapolating plots of  $I_F$  against (added  $[\text{Br}_2]$ ) or (added  $[\text{Cl}_2]$ ). In these cases, within the admittedly considerable scatter of the results (fig. 4), no significant difference between endpoints measured by the  $\text{F} + \text{Cl}_2$  and  $\text{F} + \text{Br}_2$  reactions could be detected.

### F ATOM RESONANCE ABSORPTION

Observation of F atom resonance absorption by both  $\text{F } 2p^5 \text{ } ^2P_{3/2}$  ground state atoms, and by  $J$ -excited  $\text{F } 2p^5 \text{ } ^2P_{1/2}$  atoms, has been reported briefly by us previously.<sup>5</sup> It was necessary to use relatively high F atom concentrations ( $\sim 10^{14} \text{ cm}^{-3}$ ) in the

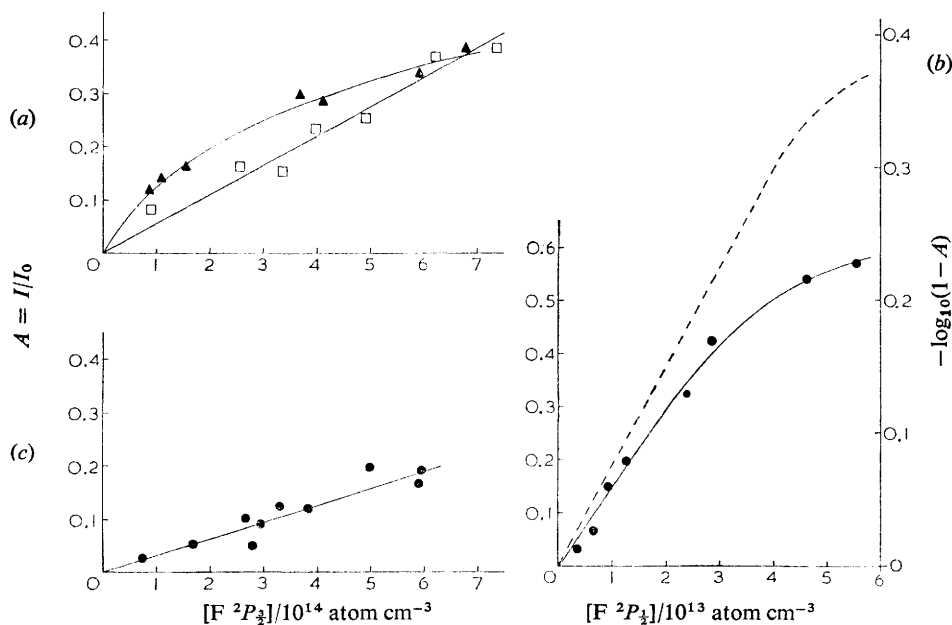


FIG. 5.—Variation of resonance absorption intensity with  $[\text{F}]$  for several transitions. (a)  $\text{F } ^2P_{3/2}$  absorption at  $\lambda$ : ▲, 95.48 nm and □, 95.19 nm; (b)  $\text{F } ^2P_{3/2}$  absorption at  $\lambda$  95.85 nm; (c)  $\text{F } ^2P_{3/2}$  absorption at  $\lambda$  97.39 nm. Broken line in (b) is a Beer-Lambert law plot for the  $\lambda$  95.85 nm absorption.

resonance lamp in order to obtain adequate intensity of the fluorine atom resonance lines, which led to strong reversal of those lines having the highest oscillator strengths  $f_{ik}$ , i.e., the  $3s \text{ } ^2P_J - 2p^5 \text{ } ^2P_J$  multiplet. As expected, therefore, the sensitivity of resonance absorption for detection of  $\text{F } 2p^5 \text{ } ^2P_J$  atoms was low. All three lines of the  $^2P_J - ^2P_J$  multiplet which were investigated showed resonance absorption [fig. 5(a), (b)].



TABLE 1.—WAVELENGTHS AND TRANSITION PROBABILITIES FOR SELECTED  $(n+1)s-np^5$  TRANSITIONS OF F, Cl, Br AND I

	F 3s			Cl 4s		
	$2P_{3/2}$	$2P_{1/2}$	$4P_{3/2}$	$2P_{3/2}$	$2P_{1/2}$	$4P_{3/2}$
$np^5\ 2P_{3/2}$						
$\lambda/\text{nm}$	95.483	95.187	97.390	134.724	133.572	137.953
$(E_k-E_i)/\text{cm}^{-1}\ ^a$	104 731	105 056	102 680	74 221	74 861	72 484
$f_{ik}$	—	—	$4.0\times 10^{-5b}$	$1.14\times 10^{-1c}$	$2.33\times 10^{-2c}$	$3.1\times 10^{-3c}$
$A_{ki}/\text{s}^{-1}$	—	—	$3.5\times 10^5$	$4.19\times 10^8$	$1.74\times 10^8$	$1.1\times 10^7$
$np^5\ 2P_{1/2}$						
$\lambda/\text{nm}$	95.852	95.555	97.775	136.345	135.166	139.653
$(E_k-E_i)/\text{cm}^{-1}$	104 327	104 652	102 276	73 340	73 980	71 603
$f_{ik}$	—	—	$1.0\times 10^{-5b}$	$4.2\times 10^{-2c}$	$8.8\times 10^{-2c}$	$8.8\times 10^{-4c}$
$A_{ki}/\text{s}^{-1}$	—	—	$4.4\times 10^4$	$7.5\times 10^7$	$3.2\times 10^8$	$1.5\times 10^6$
	Br 5s			I 6s		
	$2P_{3/2}$	$2P_{1/2}$	$4P_{3/2}$	$2P_{3/2}$	$2P_{1/2}$	$4P_{3/2}$
$np^5\ 2P_{3/2}$						
$\lambda/\text{nm}$	148.861	145.004	154.082	178.276	158.361	161.760
$(E_k-E_i)/\text{cm}^{-1}$	67 177	68 964	64 901	56 093	63 187	61 820
$f_{ik}$	$6.1\times 10^{-2d}$	$2.0\times 10^{-2}$	$6.1\times 10^{-2d}$	$1.2\times 10^{-1}$	$3.9\times 10^{-2}$	$5.3\times 10^{-2}$
$A_{ki}/\text{s}^{-1}$	$1.8\times 10^8$	$1.3\times 10^8e$	$1.7\times 10^8$	$2.56\times 10^8d$	$2.07\times 10^8e$	$1.34\times 10^8e$
$np^5\ 2P_{1/2}$						
$\lambda/\text{nm}$	157.500	153.190	163.357	206.229	179.909	184.445
$(E_k-E_i)/\text{cm}^{-1}$	63 492	65 279	59 745	48 490	55 584	54 217
$f_{ik}$	$1.5\times 10^{-2d}$	$7.1\times 10^{-2}$	$1.3\times 10^{-2d}$	$3.8\times 10^{-3}$	$1.0\times 10^{-1}$	$7.1\times 10^{-3}$
$A_{ki}/\text{s}^{-1}$	$2.0\times 10^7$	$2.0\times 10^8$	$1.7\times 10^7$	$2.96\times 10^6e$	$2.11\times 10^8e$	$6.92\times 10^6e$

<sup>a</sup> transition energies from ref. (18b); <sup>b</sup> this work; <sup>c</sup> ref. (20), which is based on data of ref. (21) and (22); <sup>d</sup> mean values from ref. (21) and (27) [see ref. (27) for discussion of data]; <sup>e</sup> ref. (21).

TABLE 2.—KINETICS OF THE F+Br<sub>2</sub> REACTION AT 300 K

[F] <sub>0</sub> /10 <sup>12</sup> cm <sup>-3</sup>	[Br <sub>2</sub> ] <sub>0</sub> /10 <sup>12</sup> cm <sup>-3</sup>	$k'/\text{s}^{-1} = -d \ln [F]/dt$		$k_1/10^{-10} \text{ cm}^3 \text{ molecule}^{-1} \text{ s}^{-1}$	
		A	B	A	B
1.2	8.75	420	514	0.51	0.74
1.6	6.11	264	434	0.48	0.79
1.0	3.12	181	269	0.66	0.98
1.3	4.88	690	895	1.58	2.05
1.3	4.06	474	693	1.34	1.96
1.4	3.46	366	552	1.26	1.90
1.4	2.53	320	468	1.64	2.40
1.2	2.88	404	474	1.68	1.97
1.2	3.51	359	535	1.18	1.76
1.5	4.39	312	476	0.82	1.25
1.7	4.80	417	615	1.01	1.49
1.4	5.11	327	536	0.72	1.18
1.3	3.95	308	486	0.90	1.42
1.2	4.62	375	536	0.91	1.30
1.1	5.01	385	577	0.84	1.26
1.3	5.45	379	515	0.77	1.25
1.0	6.07	284	409	0.50	0.72
mean values				0.90	1.44

A; preliminary measurement of  $k_1$  based on  $I_F \propto [F^2P_J]$ . B; measurement of  $k_1$  using correction for self-reversal of F atom resonance fluorescence (see text).



Fig. 5 shows that the  $^2P_{3/2}-^2P_{1/2}$  transition (at 95.85 nm) showed a higher sensitivity to F  $^2P_{3/2}$  atoms in resonance absorption than the sensitivity to F  $^2P_{1/2}$  atoms of either the  $^2P_{3/2}-^2P_{3/2}$  transition (at 95.48 nm) or the  $^2P_{3/2}-^2P_{1/2}$  transition (at 95.19 nm). Because the Boltzmann population of F  $^2P_{1/2}$  atoms at the lamp temperature ( $\sim 600$  K),  $[F\ ^2P_{1/2}]/([F\ ^2P_{3/2}] + [F\ ^2P_{1/2}])$ , was only 0.18, the strong 95.85 nm  $^2P_{3/2}-^2P_{1/2}$  line was less reversed than the strong 95.48 nm  $^2P_{3/2}-^2P_{3/2}$  line, hence leading to a relatively high integrated absorption coefficient for the 95.85 nm line.<sup>17</sup> Plots of fractional absorption,  $A$ , against  $[F\ ^2P_{3/2}]$  are shown in fig. 5(a). These plots showed a greater curvature for the 95.48 nm transition than for the 95.19 nm transition, and comparable sensitivities for both lines, again consistent with the expected self-reversal in the lamp. Table 1 shows values for the oscillator strengths for the analogous transitions of Cl and Br, from which ratios of oscillator strengths  $[f_{ik}(^2P_{3/2}-^2P_{3/2})]/[f_{ik}(^2P_{3/2}-^2P_{1/2})]$  equal to 4.9 for Cl<sup>20</sup> and 3.9 for Br<sup>21</sup> are derived. This analogy with Cl and Br,<sup>20-23</sup> and simple theoretical considerations,<sup>24</sup> thus suggest that the  $^2P_{3/2}-^2P_{3/2}$  transition of F would have a higher oscillator strength (by a factor of about 4) than the  $^2P_{3/2}-^2P_{1/2}$  transition of F. This in turn is consistent with greater self-reversal in the lamp of the former transition. Similar conclusions follow from consideration of the relative emission intensities in the lamp (fig. 3) of the pairs of lines originating from the excited  $3s\ ^2P_{3/2}$  and  $3s\ ^2P_{1/2}$  states and terminating on the ground  $2p^5\ ^2P_{3/2}$  and  $2p^5\ ^2P_{1/2}$  states, i.e.,  $I(^2P_{3/2}-^2P_{3/2})/I(^2P_{3/2}-^2P_{1/2})$  and  $I(^2P_{3/2}-^2P_{3/2})/I(^2P_{1/2}-^2P_{1/2})$ .

The only  $^4P_{3/2}-^2P_{3/2}$  transition investigated, the  $^4P_{3/2}-^2P_{3/2}$  line at 97.39 nm, showed weak resonance absorption [fig. 5(c)], but the corresponding  $^4P_{3/2}-^2P_{1/2}$  line at 97.77 nm showed no detectable absorption ( $A < 0.07$  with  $[F\ ^2P_{3/2}] \leq 4 \times 10^{13}\text{ cm}^{-3}$ ).

#### OSCILLATOR STRENGTHS $f_{ik}$ FOR F ATOM TRANSITIONS

The absorption measurements may be used to derive values for the oscillator strengths  $f_{ik}$  of the  $^4P_{3/2}-^2P_{3/2}$  pair of transitions as follows. The ratio of emission intensities from the F atom lamp,  $I(^4P_{3/2}-^2P_{3/2})/I(^4P_{3/2}-^2P_{1/2})$  was about 6 (fig. 3) compared with values of 7 and 10 for the ratios of Einstein coefficients  $A_{ki}$  for the same transitions of Cl and Br.<sup>19-23</sup> Consequently, reversal in our lamp of the  $^4P_{3/2}-^2P_{3/2}$ , 97.39 nm, line of F is expected to be low; and reversal of the  $^4P_{3/2}-^2P_{1/2}$ , 97.77 nm line should be negligible. For the 97.77 nm line, we thus assumed the source of resonance radiation to be a non-reversed Doppler line profile at a temperature of 600 K. (This temperature is typical of values used previously<sup>25</sup> for low-power microwave plasmas of the type used here). A simple model<sup>17, 23</sup> to convert integrated absorption,  $A$ , into the corresponding optical depth in the absorber,  $k_0l$ , leads to the result for the 97.77 nm line,  $k_0l < 0.15$  for  $N = [F\ ^2P_{3/2}] = 4 \times 10^{13}\text{ cm}^{-3}$ . With  $l = 3\text{ cm}$  and  $\Delta\nu_D = 0.29\text{ cm}^{-1}$  for the 97.77 nm line absorber, we deduced the upper limit  $f_{ik} < 4 \times 10^{-4}$  for the 97.77 nm line of F, using eqn (I):<sup>26</sup>

$$f = \frac{1}{2} \Delta\nu_D (\pi / \ln 2)^{1/2} (mc / \pi e^2) (k_0 / N). \quad (\text{I})$$

A similar procedure with similar assumptions, was used to analyse the absorption data of fig. 5(c) for the 97.39 nm  $^4P_{3/2}-^2P_{3/2}$  transition of F. This resulted in the values  $k_0l/N = 3.0 \times 10^{-16}\text{ cm}^3$  and  $f_{ik} = 3.3 \times 10^{-5}$  for this transition. Because of self-reversal in the lamp, this value of  $f_{ik}$  is a lower limit. Arguments presented above show that self-reversal of the 97.39 nm line is low. To estimate the magnitude of this self-reversal, it is assumed that the ratio of Einstein coefficients  $A_{ki}$  for 97.39 nm and 97.77 nm is 8 (the mean of the ratios quoted above for Cl and Br). The experimental lamp intensity ratio for these lines is 6, which then leads, via the usual model,<sup>17</sup> to an optical depth in the source  $k_0m \simeq 0.5$ . When this value,  $k_0m \simeq 0.5$ , is used in the model used to obtain  $k_0l$  from  $A$ , the slightly higher values  $k_0l/N = 3.5 \times 10^{-16}$

$\text{cm}^3$  and  $f_{ik} = 4.0 \times 10^{-5}$  were obtained for the 97.39 nm  $4P_{3/2} - 2P_{3/2}$  transition of F. The value  $f_{ik} = 4.0 \times 10^{-5}$  clearly cannot be regarded as an accurate measurement, but it would be most surprising if its magnitude differed from the true value by more than a factor of 2. To estimate  $f_{ik}^{97.77}$  we take, as before,  $A_{ki}^{97.39}/A_{ki}^{97.77} = 8$ , i.e.,  $f_{ik}^{97.39}/f_{ik}^{97.77} = 4$ . This leads to the result  $f_{ik}^{97.77} = 1.0 \times 10^{-5}$ , considerably lower than the upper limit value of  $4 \times 10^{-4}$  deduced at the beginning of this section.

In the determination of oscillator strengths from absorption measurements, it is necessary to consider the hyperfine structure of the resonance lines. In the case where the hyperfine components have a wavenumber spacing greater than, or comparable to, the Doppler width of the line,  $\Delta\nu_D$ , neglect of hyperfine splitting leads to a significant under-estimate of  $f_{ik}$ .<sup>27</sup> Fig. 6 shows the nuclear hyperfine structures of the 97.39 nm

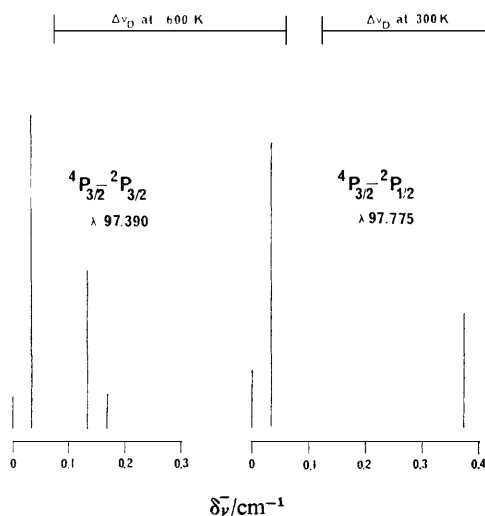


FIG. 6.—Nuclear hyperfine structure of the  $3s\ 4P_{3/2} - 2p^5\ 2P_{3/2}$  transitions of  $^{19}\text{F}$ . Wavenumber splitting data for ground states from ref. (30, 31) and for excited state from ref. (18b). Relative intensities within multiplets from ref. (30) on the assumption of a Russell-Saunders coupling scheme for the states involved. The line centres are shown in the figure.

and the 97.77 nm lines of  $^{19}\text{F}$ , which have been calculated from the results of Lidén,<sup>18b</sup> Harvey<sup>28</sup> and Radford, Hughes and Beltran-Lopez.<sup>29</sup> Each energy level of  $^{19}\text{F}$  is doubled ( $F = J \pm \frac{1}{2}$ ) on account of the nuclear spin ( $I = \frac{1}{2}$ ). The  $4P_{3/2} - 2P_{3/2}$  (97.39 nm) transition is a quartet consisting of two close pairs of lines; the overall width of the quartet,  $0.168\ \text{cm}^{-1}$ , is less than half the Doppler width of  $^{19}\text{F}$  at 600 K ( $\Delta\nu_D = 0.412\ \text{cm}^{-1}$ ). The overall width of the quartet is also less than  $\Delta\nu_D$  at 300 K for the absorbing  $\text{F}\ 2P_{3/2}$  atoms. In view of the approximate nature of the measurements of  $f_{ik}$  here, no correction to  $f_{ik}$  (97.39) for hyperfine structure is thought to be necessary. On the other hand, the overall width,  $0.375\ \text{cm}^{-1}$ , of the triplet formed by the  $4P_{3/2} - 2P_{1/2}$  (97.77 nm) transition, is comparable to  $\Delta\nu_D$  even at 600 K. Consideration of the wavenumber separations and relative intensities<sup>30</sup> of the components of the triplet (fig. 6) shows that the 97.77 nm transition for the 300 K absorber will appear as a partially resolved doublet with relative intensities of 3 : 1. However, since  $f_{ik}$  (97.77) was estimated from the relevant emission intensity ratio, rather than from line absorption, no correction to the value  $f_{ik}$  (97.77) =  $1.0 \times 10^{-5}$  is required.

These values of  $f_{ik}$  for the  $4P_{3/2} - 2P_{3/2}$  transition of F appear to be the first published data. They fit in well with the trend established for the  $4P_{3/2} - 2P_{3/2}$  transitions by the

series Cl, Br, I (see table 1). Due to increasing breakdown of the spin selection rule as a function of increasing atomic mass,<sup>24</sup> the  $f_{ik}$  values for the spin-disallowed  $(n+1)s^4P_{\frac{3}{2}}-np^5\ ^2P_{\frac{3}{2},\frac{1}{2}}$  transitions increase markedly (by  $\sim 10^3$  to  $10^4$ ) in going up the series from F to I. The magnitudes of  $f_{ik}$  for the  $3s\ ^4P_{\frac{3}{2}}-2p^5\ ^2P_{\frac{3}{2},\frac{1}{2}}$  transitions of F are similar to those for the spin-forbidden  $(n+1)s\ ^5S-np^4\ ^3P_J$  transitions of sulphur, and greater than those for the same transition of oxygen,<sup>20</sup> as would also be expected.

$f_{ik}$  for the  $3s\ ^4P_{\frac{3}{2}}-2p^5\ ^2P_{\frac{3}{2}}$  transition is between  $10^3$  and  $10^4$  times less than that expected for the  $3s\ ^2P_{\frac{3}{2}}-2p^5\ ^2P_{\frac{3}{2}}$  transition (i.e., about 0.1-0.5), and the radiative lifetime for the  $3s\ ^4P_{\frac{3}{2}}$  excited state is deduced from our  $f_{ik}$  data to be 2.3  $\mu$ s. The relatively high emission intensity from the lamp of the  $3s\ ^4P_J-2p^5\ ^2P_J$  multiplet, compared with the  $3s\ ^2P_J-2p^5\ ^2P_J$  multiplet (fig. 3), is surprising, in view of the presumed susceptibility of the long-lived  $3s\ ^4P_J$  states to electronic quenching. In that context, we note that the radiative lifetimes of the  $^4P_{\frac{3}{2}}$  and  $^4P_{\frac{1}{2}}$  states of the  $3s$  configuration are likely to be considerably longer than the value of 2.3  $\mu$ s estimated for  $^4P_{\frac{3}{2}}$ . Analogy with the  $4s\ ^4P_J$  states of Cl<sup>20, 22</sup> suggests lifetimes of the order of 10  $\mu$ s for F  $3s\ ^4P_{\frac{3}{2}}$  and the order of 100  $\mu$ s for F  $3s\ ^4P_{\frac{1}{2}}$ . Nevertheless, emission from both these excited states in the lamp was quite intense (fig. 3). It appears that for F, as for Cl and Br,<sup>19, 23</sup> formation of the lowest energy  $^4P_J$  multiplets of the  $ns$  configuration is strongly preferred in microwave excitation with He carrier gas. For Cl and Br, a similar propensity to populate the lowest energy atomic states is found in the collision of He  $2^3S_1$  metastable atoms with Cl<sub>2</sub> and Br<sub>2</sub>.<sup>31</sup>

## F ATOM RESONANCE FLUORESCENCE

A preliminary survey showed weak resonance fluorescence due to both the  $^2P_J-^2P_J$  and the  $^4P_J-^2P_J$  multiplets of F. The intensity of the fluorescence (with  $[F\ ^2P_{\frac{3}{2}}] \sim 5 \times 10^{14}\text{ cm}^{-3}$ ) was then maximized by increasing the microwave lamp power to 70 W, and by increasing the flow rate (mol fraction) of F<sub>2</sub> in the F<sub>2</sub>+He lamp. These changes obviously led to greater self-reversal of the F atom lines emitted from the lamp than those shown in fig. 3 and used for the resonance absorption studies.

Fig. 7 shows the spectrum of F atom resonance fluorescence, excited in a concentration of F  $^2P_J$  atoms of  $3 \times 10^{14}\text{ cm}^{-3}$ , with resolution of 0.2 nm (100  $\mu$ m spectrometer slits). As expected from the resonance absorption results and the above discussion of  $f_{ik}$  values, the major intensity of resonance fluorescence was emitted in the  $^2P_J-^2P_J$  multiplet, with the  $^2P_{\frac{3}{2}}-^2P_{\frac{1}{2}}$  95.85 nm line as the most intense single feature ( $\sim 11$  Hz of detected photoelectron flux rate). The relative weakness of the strong  $^2P_{\frac{3}{2}}-^2P_{\frac{3}{2}}$  95.48 nm transition in resonance fluorescence (fig. 7) is noted. This is undoubtedly due to extensive self-reversal of 95.48 nm resonance fluorescence at  $[F\ ^2P_J] = 3 \times 10^{14}\text{ cm}^{-3}$ , since the ratio of Einstein coefficients for spontaneous emission,  $A_{ki}(95.48)/A_{ki}(95.85)$ , is of the order of 5-10 (by analogy with Cl).<sup>20</sup> The relative intensities of transitions in fluorescence broadly parallel those in absorption, with little light being emitted in the spin-forbidden  $^4P_J-^2P_J$  multiplet. Fig. 8(a) and (b) show the dependences of the weak fluorescence intensities,  $I_F$ , at 95.85 nm and 97.39 nm upon  $[F\ ^2P_J]$ , using the F+Cl<sub>2</sub> reaction to determine  $[F\ ^2P_J]$ . The detected photoelectron flux rates were too low, with  $[F\ ^2P_J] < 5 \times 10^{13}\text{ cm}^{-3}$ , for systematic measurements.

Because of their weakness, the  $^4P_J-^2P_J$  multiplet transitions were not investigated further. Attention was directed to maximizing the detected fluorescence in the  $^2P_J-^2P_J$  transitions, by increasing the spectrometer slit width to 1 mm, centred on the 95.85 nm line. This spectrometer band width, about 2 nm, now allowed transmission of fluorescence due to the entire  $^2P_J-^2P_J$  multiplet. Fig. 8(c) shows the resulting

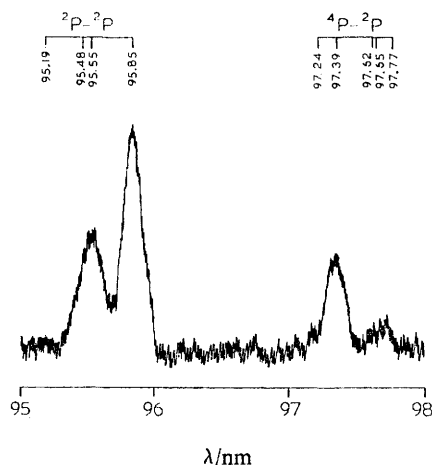


FIG. 7.—Spectrum of F atom resonance fluorescence.  $[F\ ^2P_J] = 3 \times 10^{14}\text{ cm}^{-3}$ ; 100  $\mu\text{m}$  slits. Observed photon flux rate of 95.85 nm line = 11 Hz. Note the relatively high intensity of the  $4P_{3/2}-2P_{3/2}$  97.39 nm line, due to very strong reversal (and loss of intensity) of the  $2P_J-2P_J$  lines with  $[F] = 3 \times 10^{14}\text{ cm}^{-3}$ .

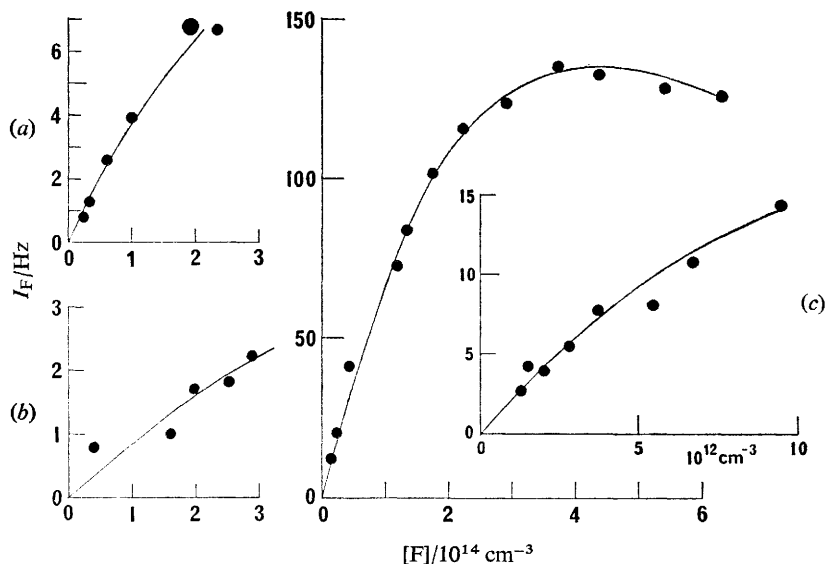


FIG. 8.—F atom resonance fluorescence. Variation of  $I_F$  with  $[F\ ^2P_J]$  for various transitions. (a)  $\lambda\ 95.85\text{ nm}$ ,  $3s\ ^2P_{3/2}-2p^5\ ^2P_{3/2}$ ; (b)  $\lambda\ 97.39\text{ nm}$ ,  $3s\ ^4P_{3/2}-2p^5\ ^2P_{3/2}$ ; (c) entire  $3s\ ^2P_J-2p^5\ ^2P_J$  multiplet. Inset shows measurements at low  $[F\ ^2P_J]$ .

variation of  $I_F$  with  $[F\ ^2P_J]$  over a wide concentration range ( $0.01$  to  $6.3 \times 10^{14}\text{ cm}^{-3}$ ), again using the  $F + \text{Cl}_2$  titration reaction to measure  $[F\ ^2P_J]$ . The plot of  $I_F$  against  $[F\ ^2P_J]$  [fig. 8(c)] shows an apparently linear range at the lowest  $[F\ ^2P_J]$ , and a maximum detected fluorescence count rate equal to 135 Hz at  $[F\ ^2P_J] \simeq 4 \times 10^{14}\text{ cm}^{-3}$ . Above this concentration,  $I_F$  decreased slightly with increasing  $[F\ ^2P_J]$ . This behaviour is analogous to that found previously for oxygen atom resonance fluorescence,

$O\ 3s\ ^3S_1-2p^4\ ^3P_J$ .<sup>17</sup> It is consistent with the onset of self-reversal of fluorescence at relatively low  $[F\ ^2P_J]$ , followed by radiation trapping and quenching of excited atoms at high  $[F\ ^2P_J]$ .<sup>17</sup>

In order to establish the variation of  $I_F$  with  $[F\ ^2P_J]$  at lower concentrations ( $<1 \times 10^{13}\text{ cm}^{-3}$ ), the background count rate (dark count + scattered light count) was reduced from 4 Hz to 2.5 Hz by cooling the photomultiplier (see Experimental). Also, the  $F + Br_2$  reaction was used to measure  $[F\ ^2P_J]$ , for the reasons mentioned earlier regarding measurements of low F atom concentrations. This calibration of  $I_F$  against  $[F\ ^2P_J]$  [inset of fig. 8(c)] was carried out in the concentration range  $1.3 \times 10^{12} \leq [F\ ^2P_J] \leq 9.4 \times 10^{12}\text{ cm}^{-3}$ . The onset of curvature on the plot [fig. 8(c)] is difficult to locate because of the inevitably large statistical scatter of the low counts measured, but it appears to occur below  $2 \times 10^{12}\text{ cm}^{-3}$ , as would be expected (see below).

The lowest concentration of  $[F\ ^2P_J]$  that could be measured in this way by resonance fluorescence was limited by the magnitude of the corresponding photoelectron count rate. The detection system showed evidence of only infrequent interference spikes. In the absence of such spikes, and using an integrating time of 50 s to count photoelectrons, the minimum measureable count rate (with signal-to-noise of unity) was 0.2 Hz. The corresponding  $F\ ^2P_J$  atom concentration was  $\sim 7 \times 10^{10}\text{ cm}^{-3}$ , so a conservative lower limit of detection would be  $[F\ ^2P_J] > 1 \times 10^{11}\text{ cm}^{-3}$ . We emphasize that this limit could be severely degraded upwards by appreciable rf interference or by drift in the photomultiplier dark count due to temperature variations in its photocathode, which were minimized in our work (see Experimental).

#### RATE CONSTANT $k_1$ FOR THE REACTION $F + Br_2 \xrightarrow{k_1} BrF + F$

Detection of  $F\ ^2P_J$  atoms by resonance fluorescence was used to measure the rate of their reaction with molecular bromine. Because of the high magnitude of  $k_1$  and because of the limited sensitivity of F atom resonance fluorescence, the range of conditions for the kinetic study was limited. The range of initial  $[F\ ^2P_J]$  was 0.98 to  $1.70 \times 10^{12}\text{ cm}^{-3}$ , and initial  $[Br_2]_0$  was between 2.5 and  $8.8 \times 10^{12}\text{ cm}^{-3}$ . The  $[Br_2]_0/[F\ ^2P_J]_0$  stoichiometry ranged between 1.8 and 7.3 with a median value of 4. Pseudo first-order kinetic analysis was used, eqn (II), with correction for  $Br_2$  consumption during the reaction,

$$\ln([F]_0/[F]) = k_1([Br_2]_{\text{mean}})t. \quad (\text{II})$$

To obtain values for  $k_1$ , the assumption was made initially that  $I_F \propto [F\ ^2P_J]$  over the F atom concentration range used; this assumption is considered below.

Fig. 9 shows typical first order decay plots for attenuation of F atom resonance fluorescence in the presence of  $Br_2$ . The scatter of the results, due to the low count rates measured, was much greater than that observed in similar Cl atom kinetic studies using resonance fluorescence.<sup>19</sup> 17 independent runs were made and the results are summarized in table 2. Data reduction was carried out computationally, with a least mean squares fitting program, which allowed for any drift (usually  $<10\%$ ) in initial  $[F\ ^2P_J]$  concentration. The mean value obtained for  $k_1$ , on the assumption of proportional dependence of  $I_F$  upon  $[F\ ^2P_J]$ , was  $(0.9 \pm 0.2) \times 10^{-10}\text{ cm}^3\text{ molecule}^{-1}\text{ s}^{-1}$  at 300 K. Several of the experimental difficulties have already been referred to, including the presence of  $O\ ^3P_J$  atoms whose concentrations are estimated to be  $\sim 0.1 [F\ ^2P_J]$ . Removal of these  $O\ ^3P_J$  atoms by addition of  $NO_2$  as scavenger was found to be not feasible, because addition of  $NO_2$  considerably increased reaction of F atoms with the walls. Since  $O\ ^3P_J$  atoms react fairly rapidly with  $Br_2$ , it is possible that our value of  $k_1$ , which neglects such reaction, is a slight underestimate.

A more serious cause for underestimation of  $k_1$  is self-reversal of resonance fluorescence. The following considerations show that such self-reversal is not negligible, even in the range of  $\sim 10^{12} \text{ cm}^{-3}$  used for typical  $[\text{F } ^2\text{P}_J]_0$ . The dominant transitions contributing to the detected fluorescence are the  $^2\text{P}_{3/2}-^2\text{P}_{3/2}$  line at 95.48 nm and the  $^2\text{P}_{3/2}-^2\text{P}_{1/2}$  line at 95.85 nm (cf. fig. 6). Since  $A_{ki}$  for the 95.48 nm line is probably between five and ten times greater than that for the 95.85 nm line (see above), the 95.48 nm line contributes the dominant intensity at sufficiently low  $\text{F } ^2\text{P}_J$  concentrations. As  $[\text{F } ^2\text{P}_J]$  is increased, the  $^2\text{P}_{3/2}-^2\text{P}_{3/2}$  95.48 nm line becomes strongly self-reversed while the  $^2\text{P}_{3/2}-^2\text{P}_{1/2}$  95.85 nm line is little affected, because  $[\text{F } ^2\text{P}_{3/2}]/([\text{F } ^2\text{P}_{3/2}] + [\text{F } ^2\text{P}_{1/2}])$  is only 0.07 at 300 K. Hence, at high  $[\text{F } ^2\text{P}_J]$ , e.g., about  $10^{14} \text{ cm}^{-3}$ , the 95.85 nm line is much more intense than the 95.48 nm line in resonance fluorescence.

This simple concept was used to set up a model for the variation of  $I_F$  with  $[\text{F } ^2\text{P}_J]$  in the concentration range  $< 2 \times 10^{12} \text{ cm}^{-3}$ , assuming that the only emitter was the  $\text{F } 3s \text{ } ^2\text{P}_{3/2}$  state referred to above. The further assumption was made that the oscillator strengths  $f_{ik}$  for the  $^2\text{P}_{3/2}-^2\text{P}_{3/2}$  lines of F were the same as those for the similar transition of Cl (see table 1 for values). Clyne and Townsend,<sup>23</sup> among others, have described a method for relating integrated line absorption, with an optically-thin Döppler source, to the corresponding value for  $f_{ik}$ . The same computer programs<sup>23</sup>

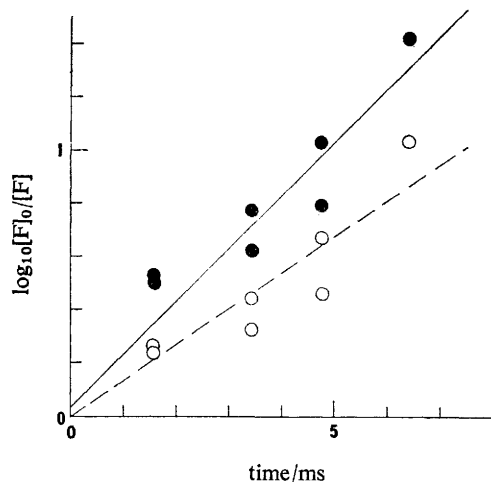


FIG. 9.—Kinetics of the  $\text{F} + \text{Br}_2$  reaction using fluorine atom resonance fluorescence. Typical data for F atom decay are shown in the form of a first order plot.  $[\text{Br}_2]_0 = 4.39 \times 10^{12} \text{ cm}^{-3}$ ;  $[\text{F}]_0 = 1.51 \times 10^{12} \text{ cm}^{-3}$ . ○ and broken line show results of preliminary analysis, assuming  $I_F \propto [\text{F } ^2\text{P}_J]$  (see text). ● and full line show results of final analysis allowing for reversal of fluorescence (see text).

were used to form a polynomial function relating  $I_F$  to  $[\text{F } ^2\text{P}_J]$ . This polynomial function did not approximate well to a straight line above  $[\text{F } ^2\text{P}_J] = 3 \times 10^{11} \text{ cm}^{-3}$ , indicating that correction for self-reversal to  $I_F$  at higher values of  $[\text{F } ^2\text{P}_J]$  was indeed required. The polynomial was used in an iterative routine to obtain improved values of  $[\text{F } ^2\text{P}_J]$  corresponding to each measured  $I_F$ . The new values for  $[\text{F } ^2\text{P}_J]$  for each kinetic run were then reanalysed computationally, as before, to give first order ( $-\text{d} \ln [\text{F}]/\text{d}t$ ) and second order ( $k_1$ ) rate constants. The results are given in table 2. The mean value for  $k_1$  from the improved data reduction procedure was  $(1.4 \pm 0.3) \times 10^{-10} \text{ cm}^3 \text{ molecule}^{-1} \text{ s}^{-1}$ .

The main error in this corrected value for  $k_1$  was introduced by the uncertainty in the oscillator strength for the 95.48 nm line,  $\text{F } ^2\text{P}_{3/2}-^2\text{P}_{3/2}$ . Therefore, the calculation



of  $k_1$  allowing for self-reversal of resonance fluorescence, was rerun using  $f_{ik}(95.48) = 0.228$  and  $f_{ik}(95.85) = 0.084$ , i.e., exactly twice those used in the above calculation which gave  $k_1 = (1.4 \pm 0.3) \times 10^{-10} \text{ cm}^3 \text{ molecule}^{-1} \text{ s}^{-1}$ . The mean value for  $k_1$ , using  $f_{ik}(95.48) = 0.228$  and  $f_{ik}(95.85) = 0.084$ , was determined to be  $k_1 = (1.6 \pm 0.4) \times 10^{-10} \text{ cm}^3 \text{ molecule}^{-1} \text{ s}^{-1}$ . The value for  $k_1$ , corrected for self-reversal, therefore is not sensitively dependent upon the magnitude of  $f_{ik}$ . The most probable value for  $f_{ik}(95.48)$  is considered to be around 0.1 to 0.15, so the best estimate of  $k_1$  that allows for some additional error due to the uncertainty in  $f_{ik}(95.48)$  is  $k_1 = (1.4 \pm 0.5) \times 10^{-10} \text{ cm}^3 \text{ molecule}^{-1} \text{ s}^{-1}$  at 300 K.

This value for  $k_1$  may be compared with that reported by Appelman and Clyne,<sup>9</sup> using mass spectrometric analysis in a fast flow system to measure the rate of consumption of  $\text{Br}_2$  in the presence of excess F;  $k_1 = (3.1 \pm 0.9) \times 10^{-10} \text{ cm}^3 \text{ molecule}^{-1} \text{ s}^{-1}$  at 298 K. As in the present study, the extreme rapidity of reaction (1) severely restricted the maximum stoichiometry  $[\text{F}]_0/[\text{Br}_2]_0$  that could be used in their study.<sup>9</sup> On the other hand, the problem of irreproducible surface reaction of F at the flow tube walls (see below) led to less difficulty in the mass spectrometric work. This is because F atom concentrations, and their decays, were determined directly through the reaction zone using mass spectrometric measurements. The presence of  $\text{O } ^3\text{P}_J$  stream would have led to an overestimate of  $k_1$  in the mass spectrometric study, by accelerating the decay of  $[\text{Br}_2]$ . However, the same impurity leads to a drop in  $-\text{d} \ln [\text{F}]/\text{d}t$  in the resonance fluorescence study. These considerations suggest that the best estimate of  $k_1$  at present is obtained by taking a mean of the two determinations, giving equal weighting to the mass spectrometric study and to the present study. The result of this procedure is  $k_1 = (2.2 \pm 1.1) \times 10^{-10} \text{ cm}^3 \text{ molecule}^{-1} \text{ s}^{-1}$  at 298–300 K.

The most useful improvement in the resonance fluorescence method for kinetic studies of  $\text{F } ^2\text{P}_J$  atom reactions would be reduction of wall reaction of F. The sensitivity of resonance fluorescence for F is sufficiently high for direct pseudo first-order kinetic studies of F atom reactions whose rate constants are as high as  $5 \times 10^{-11} \text{ cm}^3 \text{ molecule}^{-1} \text{ s}^{-1}$ . Such reactions would include  $\text{F} + \text{H}_2$ ,  $\text{F} + \text{CH}_4$  and other significant elementary processes concerned with the HF chemical laser. However, rather rapid loss of  $\text{F } ^2\text{P}_J$  atoms at the silica walls was found in our work. The rate constant for this loss process was found to be markedly affected by addition of moderate concentrations ( $> 10^{13} \text{ cm}^{-3}$ ) of many reactants (particularly  $\text{NO}_2$ ,  $\text{O}_2$ ,  $\text{O}_3$ ). Pseudo first-order kinetic analysis [eqn (I)] is only valid when first-order wall loss is unaffected by the molecular reactant, as in the  $\text{F} + \text{Br}_2$  reaction where very low concentrations of  $\text{Br}_2$  (typically  $4 \times 10^{12} \text{ cm}^{-3}$ ) were added. Future work in this laboratory will be directed towards replacing the silica surface of the flow tube by an inert teflon film,<sup>32</sup> in order to reduce (and stabilize) surface loss of  $\text{F } ^2\text{P}$  atoms.<sup>3</sup>

We thank David Gutman for introducing us to collimated hole structures. We thank the S.R.C., the Ministry of Defence and the Central Research Fund Committee of London University for support.

<sup>1</sup> A. Carrington, D. H. Levy and T. A. Miller, *J. Chem. Phys.*, 1966, **45**, 4093.

<sup>2</sup> K. H. Homann, W. C. Solomon, J. Warnatz, H. G. Wagner and C. Zetzsch, *Ber. Bunsenges. phys. Chem.*, 1970, **74**, 585.

<sup>3</sup> C. E. Kolb and M. Kaufman, *J. Phys. Chem.*, 1972, **76**, 947.

<sup>4</sup> M. A. A. Clyne, D. J. McKenney and R. F. Walker, *Canad. J. Chem.*, 1973, **51**, 3596.

<sup>5</sup> P. P. Bemand and M. A. A. Clyne, *Chem. Phys. Letters*, 1973, **21**, 555.

<sup>6</sup> D. E. Rosner and H. D. Allendorf, *J. Phys. Chem.*, 1971, **75**, 308.

<sup>7</sup> T. L. Pollock and W. E. Jones, *Canad. J. Chem.*, 1973, **51**, 2041.

<sup>8</sup> J. Warnatz, H. G. Wagner and C. Zetzsch, *Ber. Bunsenges. phys. Chem.*, 1971, **75**, 119.



- <sup>9</sup> E. H. Appelman and M. A. A. Clyne, *J.C.S. Faraday I*, 1975, **71**, 2072.
- <sup>10</sup> P. P. Bemand, M. A. A. Clyne and R. T. Watson, *J.C.S. Faraday I*, 1973, **69**, 1356.
- <sup>11</sup> P. P. Bemand, M. A. A. Clyne and R. T. Watson, *J.C.S. Faraday I*, 1974, **70**, 564.
- <sup>12</sup> See, for example, M. A. A. Clyne in *Physical Chemistry of Fast Reactions*, ed. B. P. Levitt (Plenum Press, New York, 1973), vol. 1, 245.
- <sup>13</sup> G. Schatz and M. Kaufman, *J. Phys. Chem.*, 1972, **76**, 3586.
- <sup>14</sup> J. A. Coxon, *Chem. Phys. Letters*, 1975, **33**, 136.
- <sup>15</sup> P. C. Nordine, *J. Chem. Phys.*, 1974, **61**, 224.
- <sup>16</sup> JANAF Thermochemical Tables, NSRDS-NBS 37, 2nd edn., 1970.
- <sup>17</sup> Similar considerations for  $2p^4\ ^3P_J$  oxygen atoms have been discussed by P. P. Bemand and M. A. A. Clyne, *J.C.S. Faraday II*, 1973, **69**, 1643.
- <sup>18</sup> (a) C. E. Moore, *Atomic Energy Levels*, vol. 1, NBS Circular 467, 1949; (b) K. Lidén, *Arkiv Fysik*, 1949, **1**, 229; (c) H. P. Palenius, *Arkiv Fysik*, 1969, **39**, 425.
- <sup>19</sup> P. P. Bemand and M. A. A. Clyne, *J.C.S. Faraday II*, 1975, **71**, 1132.
- <sup>20</sup> W. L. Wiese, M. W. Smith and B. M. Miles, *Atomic Transition Probabilities*, vol. 2, NSRDS-NBS 22, 1969.
- <sup>21</sup> G. M. Lawrence, *Astrophys. J.*, 1967, **148**, 261.
- <sup>22</sup> W. Hofmann, *Z. Naturforsch.*, 1967, **22a**, 2097.
- <sup>23</sup> M. A. A. Clyne and L. W. Townsend, *J.C.S. Faraday II*, 1974, **70**, 1863.
- <sup>24</sup> H. G. Kuhn, *Atomic Spectra* (Longman, London, 2nd edn., 1969).
- <sup>25</sup> See, for example, D. A. Parkes, L. F. Keyser and F. Kaufman, *Astrophys. J.*, 1967, **149**, 217.
- <sup>26</sup> A. C. G. Mitchell and M. W. Zemansky, *Resonance Radiation and Excited Atoms* (Cambridge Univ. Press, 1971).
- <sup>27</sup> M. A. A. Clyne and J. Tellinghuisen, *J.C.S. Faraday II*, in press.
- <sup>28</sup> J. S. M. Harvey, *Proc. Roy. Soc. A*, 1965, **285**, 581.
- <sup>29</sup> H. E. Radford, V. W. Hughes and V. Beltran-Lopez, *Phys. Rev.*, 1961, **123**, 153.
- <sup>30</sup> E. U. Condon and G. H. Shortley, *The Theory of Atomic Spectra* (Cambridge Univ. Press, 1951).
- <sup>31</sup> L. A. Gundel, D. King, W. S. Nip, D. W. Setser and M. A. A. Clyne, to be published.
- <sup>32</sup> H. C. Berg and D. Kleppner, *Rev. Sci. Instr.*, 1962, **33**, 248.

(PAPER 5/882)